Standardized hydrogen storage module with high utilization factor based on metal hydride-graphite composites

Inga Bürger[1], Mila Dieterich[1], Carsten Pohlmann[2,3], Lars Röntzsch[2] and Marc Linder[1]

[1] *German Aerospace Center (DLR) - Institute of Engineering Thermodynamics, Thermal Process Technology, Pfaffenwaldring 38 – 40, 70569 Stuttgart, Germany*

[2] *Fraunhofer Institute for Manufacturing Technology and Advanced Materials IFAM, Branch Lab Dresden, Winterbergstraße 28, 01277 Dresden, Germany*

[3] *now at Aaqius & Aaqius, 12 Rue Vivienne, 75002 Paris, France*

Corresponding author: Inga Bürger, inga.buerger@dlr.de, +49 711 6862 492, fax: +49 711 6862 632

Graphical Abstract

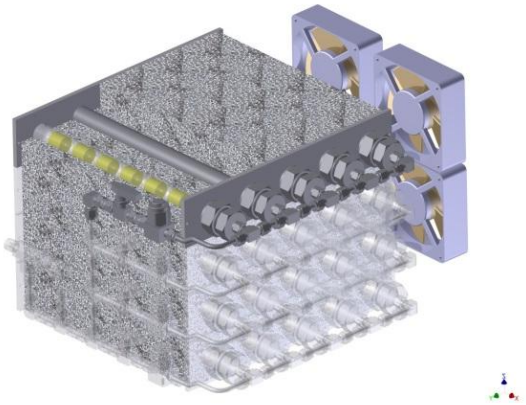

Abstract

In view of hydrogen based backup power systems or small-scale power2gas units, hydrogen storages based on metal hydrides offer a safe and reliable solution. By using Hydralloy C5 as suitable hydride forming alloy, the present tank design guarantees very simple operating conditions: pressures between 4 bar and 30 bar, temperatures between 15 °C and 40 °C and minimal efforts for thermal management in combination with fast and constant charging and discharging capabilities. The modular tank consists of 4 layers with 5 reactor tubes each that are filled with metal hydride-graphite composites of a diameter of 21 mm. Experiments show that each layer of this tank is able to desorb the desired amount of hydrogen for a fuel cell operation at electrical power of 160 W_{el} for 100 min reaching a utilization factor of 93 % of the stored hydrogen at RC. Furthermore, the experimental results of modularity, increasing loads and the electric air ventilation are presented.

Keywords

Metal hydride, stationary application, reactor design, metal hydride-graphite composites

1 Introduction

Increasing availability of devices that convert renewable energy into electricity like photovoltaic modules or wind turbines create the need for energy buffers in order to match energy availability and energy needs. For remote or decentralized power supply, one promising option is to convert electricity to chemical energy in form of hydrogen gas [1]. This allows a separate dimensioning of power and capacity, immense cyclic use without degradation as well as different options to re-use the energy on demand. An example of such a system is depicted in Figure 1. In this case, the surplus electricity converted from a fluctuating renewable energy source is used for hydrogen production by an electrolyzer. This hydrogen is then stored in a buffer tank and can be later used for different energy services such as electricity and heat via fuel cells, heat for cooking via catalytic burners and potentially also mobility.

Figure 1: Scheme of a hydrogen-based power2gas system to store surplus electrical power.

Suitable electrolyzer and fuel cell power demands for private domestic applications range between 600 W to 1.2 kW, and already exist on the market[1]. As hydrogen buffer tank for such systems usually either a high-pressure tank, which requires a hydrogen compressor, or a low-pressure tank is used, which requires a lot of free space[2]. In addition, pressure tanks especially at high pressures bear safety risks when bursting. Metal hydrides can lower these risks dramatically due to the chemical absorption of hydrogen inside of the solid metal. Additionally, suitable metal hydrides prove cycling stabilities in the five-figure range [2,3]. Consequently, hydrogen can be stored with highest volumetric densities (up to 150 g-H_2 per liter) at rather low pressures and an inherent safety aspect: The corresponding exo-/endothermic storage reaction between the metal (Me) and the hydrogen (H_2) to a metal hydride (MeH) can be written as

$$\mathrm{Me} + \frac{1}{2}\mathrm{H_2} \leftrightarrow \mathrm{MeH} + \Delta_R H. \quad (1)$$

[1] E.g., www.actaspa.com
[2] E.g., www.heliocentris.com

As the desorption of hydrogen is an endothermal process, any unintentional release of hydrogen is immediately decelerated due to the heat demand for desorption. However, at the same time the involved heat of reaction is most challenging when designing a metal hydride hydrogen storage. Overcoming this drawback, a simple and standardized storage design combining the advantages of metal hydrides - safe, low volume, low pressure, little maintenance, no compressor - with improved thermal transfer is proposed in this paper.

In the literature, several studies have been published focusing on metal hydride buffer tanks for stationary applications.

For example, magnesium hydride-based storage tanks are intensively studied, as this material shows very high storage capacities of up to 7.7 wt.% [4]. Due to their high operating temperature, these materials require a rather complex heat management based on a process integration [5] or e.g. the combination with a phase change material to preserve the associated thermal energy [6].

The advantages of metal hydrides working near ambient conditions for this buffer storage application is discussed by Hagstorm [7]. In this paper, it is emphasized that for the selection of a suitable material a small hysteresis as well as a flat plateau of the PCI curve are crucial, leading to the suggestion of LmNi(1)[3] (JMC[4]) or Hydralloy C15 (GfE[5]).

Lototskyy et al. also designed metal hydride reactors using an AB_2-type material as fuel cell supply tanks [8]. In that paper, the effect of different hydrogen desorption rates is discussed as well as the influence of liquid or air heat transfer on the overall performance, and for the charging process very fast rates are assumed. A similar study has been performed by Capurso et al. using Hydralloy C5 powder material in 0.5 liter containers as hydrogen storage for an urban concept car [9].

Bossi et al. tested a setup where a $LaNi_5$ based storage reactor for 6000 NL[6] hydrogen is coupled to a fuel cell fluid for stationary back-up systems [10], and Nakano et al. studied in the project THEUS a metal hydride tank that is integrated as buffer tank between an electrolyzer and a fuel cell [11]. In both cases, the hydride tank is integrated into a water based cooling/heating system, which leads to a rather complex tank design and overall system.

Furthermore, Liu et al. designed a new overall fuel cell -metal hydride hydrogen storage design for stationary applications [12]. This system show advantages for the air-cooled fuel cell due to a more direct heat management, however, in this case the capacity of the tank is linked to the size of the fuel cell.

[3] Lm = La-rich misch metal
[4] Japan Metals & Chemicals Co. Ltd.
[5] Gesellschaft für Elektrometallurgie mbH.
[6] NL = normal liter at 0 °C and 1.103 bar

Summarizing the experience of the given references, the focus of the present metal hydride tank has been on a standardized system design with a very low complexity of the thermal management. Therefore, the following points have been considered.

- A suitable low temperature metal hydride material with a low hysteresis has been chosen that can store and release hydrogen under the applying conditions of room temperature between 10 and 40 °C. Thus, no further system integration with e.g. fuel cell or water management was required.
- The power of the electrolyzer and the fuel cell were assumed to be in a similar range, thus, charging and discharging rates are similar with similar effects on the reactor design.
- The pure hydride material has been mixed with expanded natural graphite (ENG) and compressed to metal hydride-graphite composites (MHC) to improve the radial thermal conductivity. Thus, the final storage system is based on tubes with comparatively large diameter and aluminum foam on the outside to improve heat transfer and requires only simple air ventilation at low power.

For demonstration, a tank based on 4 layers with 5 tubes each, that are filled with in total 6 kg of Hydralloy C5® based MHC, has been built. The storage reactor has been designed in such a way that each layer is able to supply sufficient hydrogen to generate an electric power of 160 W by a fuel cell for more than 100 minutes. For the evaluation of the performance, a utilization factor has been defined that refers to the ratio between the “mass of hydrogen released/stored with relevant flow rates” and the “maximum mass of hydrogen that can be discharged/charged” at the corresponding operation conditions. The final goal was to show that with the presented reactor utilization factors of more than 90% can be reached.

In this paper, first, the general system layout based on Hydralloy C5® is described and the effect of the usage of MHCs with enhanced heat conductivity is presented. Then, details on the final tank and the test rig are given before the experimental results are shown concluding that this system is able to store and provide hydrogen at the required rate. Finally, the results of varying flow rates and air ventilation are presented and a summary and evaluation of the total system is discussed.

2 System layout

As mentioned in the introduction, for hydrogen storage in metal hydride systems, usually an intense thermal management is required. For the present setup, the first measure to reduce the complexity of the system is the implementation of a material that can store (absorb) and release (desorb) hydrogen under ambient conditions (between 15 °C and 40 °C). Thus, in contrast to other proposed systems [11] no further heating or cooling integration is required.

The material that has been chosen is known as Hydralloy C5 (AB_2-type metal hydride) and has been widely studied in the literature. It is stable during cycling as powder [2,13] and in form of MHC [14,15]. Additionally, it can be filled into tanks in the unactivated state without inert-gas measures and can easily be activated inside the final tank [9]. Furthermore, the kinetics of the material are fast, i.e. absorption and desorption proceed in the relevant temperature and pressure range in less than 30 s [16], and its hysteresis as well as plateau slope are moderate [9,17]. Figure 2 shows the Van´t Hoff plot for this material indicating 20 %, 50 % and 80 % transformed fraction for absorption and desorption, respectively. The arrows indicate the operational conditions for this system.

For absorption, a hydrogen supply pressure of 30 bar is assumed, as this corresponds to a reasonable pressure provided by an electrolyzer without a complementary compressor[7]. Thus, if room temperature of 15 °C to 40 °C is assumed, there is still a temperature difference of 10 K to the equilibrium of 80 % transformed fraction for absorption that can be used to remove the heat efficiently. As several typical fuel cells operate with back pressures between ambient and 200 mbar backpressure and as the expected pressure difference to the inlet pressure is only few 10s of mbar, for desorption [18], it is assumed that 4 bar correspond to a reasonable operation pressure. As can be seen in Figure 2, the equilibrium temperature at 4 bar is 5 °C, thus in this case there is a temperature difference of 10 K to provide the heat to the storage tank.

In short, it can be stated that this material fulfills the thermodynamic requirements for a metal hydride hydrogen storage allowing for a quite simple thermal management as mentioned in the introduction.

[7] E.g., www.actaspa.com

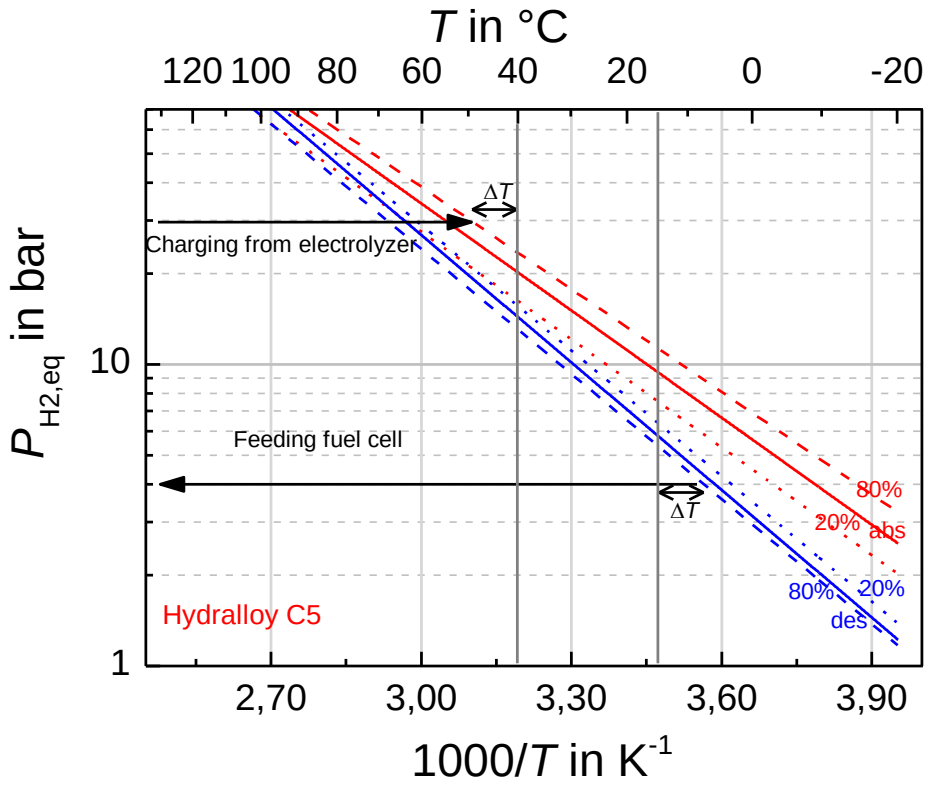

Figure 2: Van´t hoff plot of Hydralloy C5 [17]**, and operation conditions for the present reactor design.**

Next to the selection of a suitable material, also for the reactor design two aspects were considered to keep the complexity of the system low: First, air was chosen as easy to handle heat transfer fluid that is also non-toxic and abundant. Second, the design of the reactor focused on a reduced amount of reactor wall material in comparison to the metal hydride material. Therefore, the applying loads and suitable heat transfer measures were analyzed for the design.

In most studies on metal hydride tanks, the thermal management of metal hydride reactions is difficult due to fast reaction rates and large amounts of thermal energy that have to be removed. E.g. in a recent study by Lototsky et al. on a hydrogen storage tank for forklifts [19], it is necessary to remove continuously ~ 9,2 kW during 15 minutes in order to fill the tank with 0.91 kg of hydrogen. Reducing the refueling time to the required values of less than 5 min for automotive applications will further increase the required cooling power. In order to handle these high heat fluxes – especially in combination with a relatively low thermal conductivity of metal hydride beds of only approximately 1 $W(mK)^{-1}$ [20] – several options to enhance the heat transfer have been discussed in the literature extending the heat transfer area with fins, foams etc. [21,22], or minimizing the distance to the heat transfer surface by reactor design [23] as well as introducing a heat transfer secondary phase, e.g. graphite, into the storage material [24].

Even though the thermal loads of the present application are lower, the utilization of one of these well-studied measures – metal hydride-graphite composites – can still contribute significantly to the simple system layout and a reduction in overall reactor mass. This will be shown in the following basic calculation for the temperature decrease in a tubular reactor for powdery and pelletized metal hydride material.

For this calculation it is necessary to know the thermal loads that will apply during operation. Furthermore, the maximum temperature decrease that still allows a continuous operation has to be considered. If these values are known, the maximum diameter of a tubular reactor using a given material can be calculated [25]. In Table 1, the basic conditions for the reference case as well as the layout of the present system are summarized. For the desired continuous electrical power of 160 W_{el} per layer, a hydrogen mass flow rate of 2.7 10^{-3} gs^{-1} is required (assuming η_{fc} = 0.5). In order to release this amount of hydrogen, with a reaction enthalpy of $\Delta_R H$ = 28.4 $kJmol^{-1}$, 38 W of thermal energy have to be provided to the material. Thus, for a continuous supply of 100 min, at least 1.35 kg of powdery Hydralloy material (corresponding to 1.42 kg of Hydralloy-based MHC including ENG) is required. Assuming an inner diameter of the tube of 21 mm, the total reactor length for the powder material is 1.95 m whereas only 1.05 m is required for the compacted MHC. As the resulting thermal power density of the MHC is about 2 times higher than the thermal power density of the powder, it is obvious that the MHC help to make the storage system more compact. However, for the MHC it is more difficult to supply the heat of reaction due to the smaller surface area. In order to show this for the present example, the temperature profile has been calculated for MHC pellets and powder (Table 1).

Assuming a cylindrical shape with a constant temperature at the outside wall and a homogeneous heat sink due to the reaction (assumed to be independent of temperature), the occurring temperature decrease at the center of the tube can be calculated with:

$$\Delta T = \frac{1}{4\lambda} S \cdot R^2 \qquad \textbf{(2)}$$

where S is the volumetric heat sink density during the desorption reaction in Wm^{-3}, λ is the heat conductivity of the material in $W(mK)^{-1}$ and R is the radius of the tube in m.

Due to the strong influence of the thermal conductivity, the temperature drop in the powder bed is a factor 5 higher than for the MHC material (see graph in Table 1) – despite the clearly higher power density in the MHC. Thus, the advantage of MHC for a compact system is based on three facts: The material is more compact, thus a smaller volume has to be covered by external steel walls. The increased thermal conductivity enables tubes with much larger diameters while still showing homogenous reaction, and a higher temperature gradient to a simple heat transfer fluid like air is

acceptable. Especially the homogeneous reaction profile, that appears when pellets are used, is important as it also leads to a very homogeneous charging state of the material. Thus, basically all material in the reactor reacts at the same time and a high value of the utilization factor for the stored hydrogen can be achieved.

So far it has been shown that due to their high thermal conductivity, the MHC show a very homogeneous temperature profile inside of the tube although their power density is quite high (see also graph in Table 1). Thus, the performance during the desorption process is assumed to be very good although tubes with a diameter of 21 mm are used. However, even though the low ratio of outside surface to volume is good for the reduction of steel, this low ratio aggravates the heat transfer from the surface to the air. For the present setup, aluminum foam is used at the outside of the tubes resulting in a heat transfer coefficient of approximately 150 $Wm^{-2}K^{-1}$. Thus, the temperature drop from the air to the center of the MHC is dominated by a ΔT_a = 3.78 K from the air to the steel wall, while inside of the MHC the temperature gradient of ΔT_i ~0.33 K can almost be neglected. This temperature difference of ~4.1 K is acceptable for the present system, as the distance of the operational temperature to the equilibrium temperature is more than 10 K, as mentioned above.

In summary it can be stated that with Hydralloy-based MHC a simple and compact hydrogen storage system could be designed as this material can operate at ambient conditions. Due to the utilization of MHC with a high thermal conductivity, the required homogeneous temperature and transformed fraction distribution can be achieved in tubes with an inner diameter of 21 mm.

Table 1: Summary of properties for powder or MHC material as well as calculated design parameters (materials properties taken from [17]).

	Hydralloy® powder	Hydralloy®-based MHC
	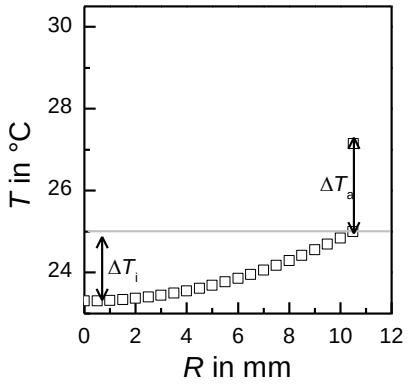	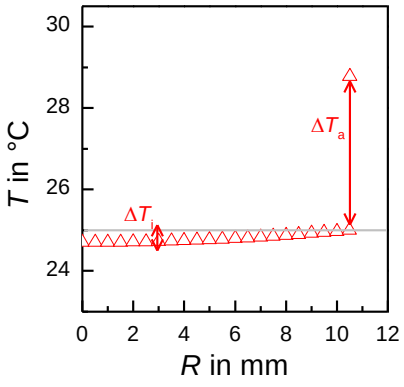
Req. power in W_{el} per layer	160	160
ρ in kgm^{-3}	2000	4040
λ in Wm^{-1}K^{-1}	1	9.9
***m* in kg**	1.35	1.42
***L* in m**	1.95	1.01
***Q/A* in Wm^{-2}**	295	567
***Q/V* in kWm^{-3}**	56.3	108.3
ΔT_i in K	1.55	0.30
ΔT_a in K	1.96	3.78

3 Experimental details

In this Section, first details on the MHC are given, then the reactor design is shown and finally the test rig is presented.

Metal hydride-graphite composites

The hydride material that has been used for the MHC is Hydralloy C5. To improve heat transfer properties, 5 wt.% of ENG were added to Hydralloy powder particles of approx. 10 µm and the mixture was compressed to composites (so-called MHC) at a pressure of 75 MPa with a diameter (*D*) to height (*H*) ratio of approximately 1.5. After compaction, a hole was drilled in the center of each MHC pellet in order to enable sufficient gas transport in axial direction. Then, the MHC pellets were filled under ambient conditions into the reactor tubes using few pieces of polyurethane foam as spacer material between the pellets to buffer the volume expansion of the MHCs [26]. In our

previous work [14], it has been shown that similar composites were geometrically stable for over 1000 cycles with a thermal conductivity of the cycled material in the range of 10 $Wm^{-1}K^{-1}$.

Reactor design

Table 2 shows a picture of the final reactor consisting of 20 stainless steel tubes with an outer diameter of 25 mm, 2 mm wall thickness and a length of about 34 cm. For the overall design, the standardized dimensions of standard 19 inch rags have been considered according to the basic idea to combine a fuel cell, standardized modular hydrogen storage and optionally an electrolyzer in one rag. Thus, the outer dimensions of the storage tank were 261 × 444 × 458 mm.

In order to enhance the heat transfer to air at the outside surface of the tubes, aluminum foam has been attached to the tubes using an adhesive paste. In addition, four small ventilators with a required electric output of 8 W_{el} were used to blow air through the foam. This prototype consists of 4 layers with 5 tubes each that can be operated separately. Furthermore, gas filters, a pressure sensor, an overpressure valve and 3 thermocouples were integrated.

It is obvious that the weight of this system with approx. 30 kg was still too heavy for a 19 inch rack solution. However, it will be possible to reduce the weight by 50 %, e.g. by replacing the fittings, as the mass of the hydride, the mass of the stainless steel tubes, and that of the foam is only 6 kg, 6.5 kg, and 1.5 kg, respectively.

Table 2: Photograph of storage tank demonstrator and its main features.

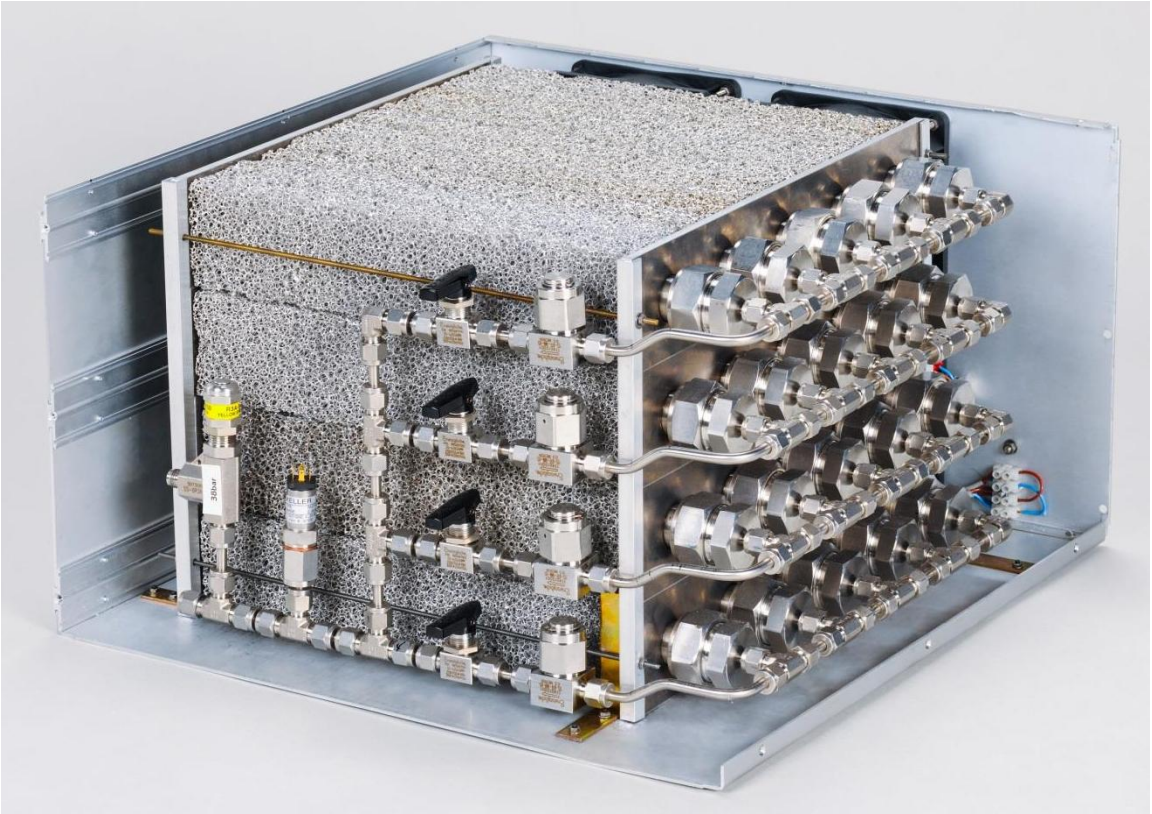

Mass MHC in kg	6
Total mass in kg	30
Stored volume of H_2 in m^3	1
Designed load in W_{el} per layer	160 for 100 min, @ 4 bar back pressure
Dimensions in mm	261 × 444 × 458

Test rig set-up

The reactor was integrated into an existing test rig (see Figure 3) that provides hydrogen at flow rates of up to 74.9 mg s^{-1} at pressures up to 100 bar to simulate the electrolysis (MFC 1). Furthermore, hydrogen can be released at constant flow rates of up to 74.9 mg s^{-1} at pressures > 10 bar using MFC 2 and at pressures < 10 bar using MFC 3, in order to simulate the hydrogen demand of a fuel cell. All mass flow controllers (MFC) have an accuracy of ± (0.5 %Rd + 0.1 % FS[8]). The pressure sensor PS1 can measure pressures up to 160 ±1.6 bar, and one thermocouple is integrated into the hydrogen supply tubes. Furthermore, another pressure sensor (PS) that is calibrated up to 40 ± 0.4 bar is integrated into the reactor. Thermocouples (Type K) have been integrated in three representative tubes. In case the pressure inside of the reactor exceeds 38 bar, an excess valve (EV) opens and the hydrogen is

[8] Rd = Reading, FS = full scale

released to the hood. In order to fully desorb the reactor it is also possible to extract the hydrogen by a vacuum pump (VP) to decrease the pressures to 0.5 mbar.

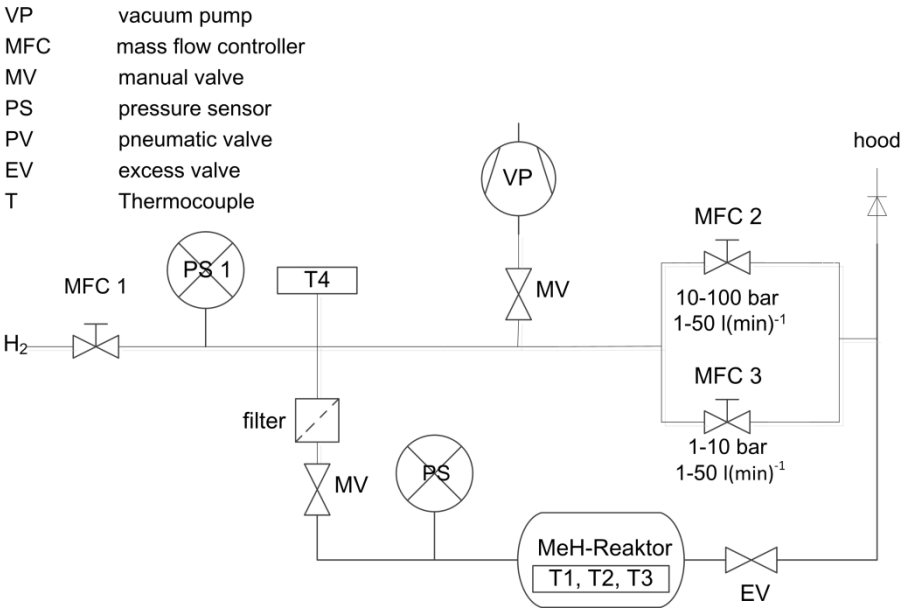

Figure 3 Test rig layout

4 Results and discussion

Preliminary to the results, in this section, the testing procedure as well as the list of experiments is presented.

The goal of the experiments was to evaluate the capability of the tank and to demonstrate that each layer of the reactor is able to store or provide sufficient hydrogen for 160 W_{el} by an electrolyzer or a fuel cell, over a time period of 100 min thereby utilizing about 90% of the storage capacity of the material at application relevant conditions. Using the dimensioning described in the previous section, this implies that - for the given charging and discharging loads - the developed storage system operates at steady-state and the temperature at the center of the reactor tubes stays almost constant during the experiment. In the reference experiment for absorption and desorption the pressure was changed between 4 and 30 bar at room temperature while keeping up a flow rate of 2.6 mgs^{-1} for at least 100 min per layer. For the complete storage (4 layers), these conditions refer to an electric fuel cell power of 640 W_{el} for 100 min (efficiency of the fuel cell: η_{fc} = 0.5).

In addition to this experiment under *reference conditions* (indicated in the following as “RC”), experimental results for the following conditions will be presented: separately operated layers (modularity), increased flow rate (factor: 2, 4, 8, (16) *RC), and an experiment without fans (effect of outside heat transfer). The absorption experiments always refer to the charging process with

hydrogen at constant flow rate from an electrolyzer, while the desorption experiments refer to the discharging process where hydrogen is provided to a fuel cell.

Reference conditions (RC)

The experiment for absorption and desorption at RC has been performed as first and last experiment of 38 experiments as well as several times in between. Figure 4 shows the mass flow rate, the pressure as well as the temperature difference profile for one experiment at the beginning (olive) and the final experiment (black) for absorption (left) and desorption (right).

As it can be seen at the top, the mass flow rate for the studied two layers has been set to a constant value of 5.2×10^{-3} gs^{-1} in order to simulate the continuous operation of an electrolyzer or a fuel cell at 320 W_{el}. This flow rate could be absorbed or desorbed from the storage for the desired 100 min. The graphs at the center of Figure 4 show the corresponding pressure profiles. In contrast to the temperature signal that is at steady-state (Figure 4, bottom), the pressure signal does not exhibit a perfectly flat plateau. This behavior has been expected as pressure-concentration-isotherms of the pure material also show a sloping plateau [17]. Furthermore, from Figure 4, for absorption, the main fraction of hydrogen is absorbed at pressures between 10 and 15 bar and for desorption between 4 and 6.5 bar. The reason for this difference is the hysteresis of the material as well as the difference in the temperature. For both experiments the initial temperature was room temperature. However, during the exothermal absorption reaction the temperature increases and reaches its steady-state approximately 5 K above room temperature, while for the endothermal desorption the temperature decreases by 5 K (based on ambient temperature). Thus, according to the thermodynamics of the material, it is reasonable that for higher temperatures a higher pressure is required.

Overall it can be stated that during the reference experiment, the behavior of the tank showed the desired steady-state behavior for 100 min, thus, the stored hydrogen can be used to a large extend (utilization factor 93%, see following section). Furthermore, during the 38 cycles the material did not show any degradation – in contrast – the material was rather continuously further activated.

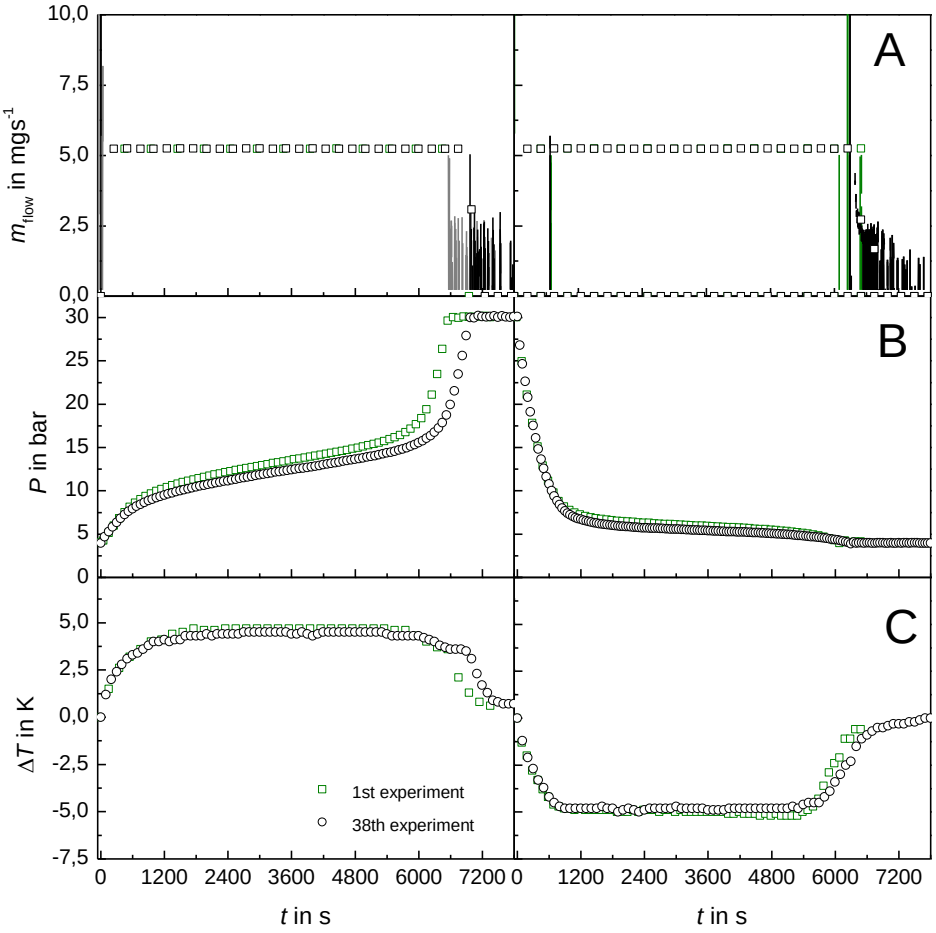

Figure 4: Mass flow rate (A), pressure (B) and temperature difference (C) versus time for absorption (left) and desorption (right) under RC.

Modularity – scale-up

After the proof of a continuous operation at steady-state, for the presented reactor it is important to show that in the modular system the single layers operate independently. This implies that for higher or lower required powers of electrolyzer or fuel cell and the same operation time, the storage reactor can be scaled up or down by simply increasing or decreasing the number of layers. Figure 5 presents the results for a continuous flow rate at 5.2 mgs^{-1} (2*RC) for layer 1 and layer 2 (triangles), furthermore the results for both layers at the double flow rate of 10.4 mgs^{-1} (2*RC – 5.2 mgs^{-1}/layer, squares). As the pressure (A) as well as the temperature signals (B), show a very good agreement, it can be concluded that the single layers are independent of each other, thus the setup can be scaled up or down regarding the loads. The temperature difference between the signals for layer 1 (open symbols) and layer 2 (closed symbols) can be explained by a slightly different position of the thermocouples inside of the reactor tubes.

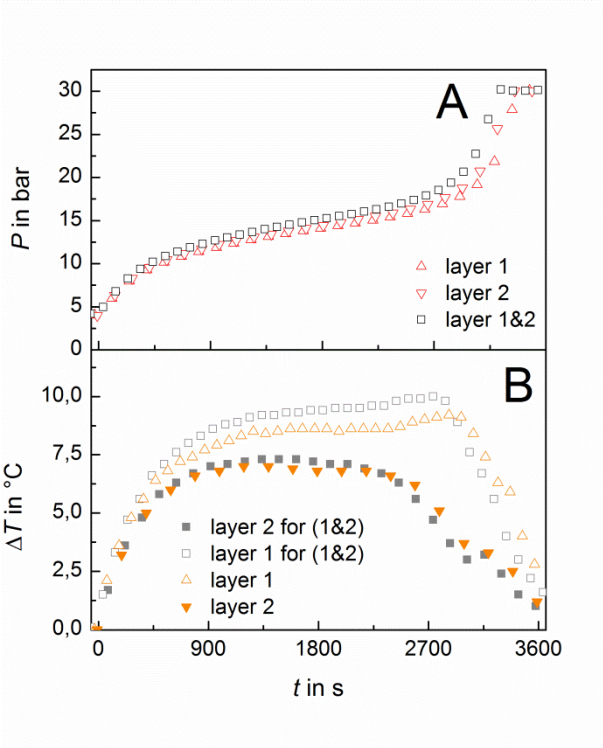

Figure 5: Pressure (A) and temperature difference (T1: full and T2: open symbols, B) versus experimental time with 2*RC and 2 layers (squares) as well as with 2*RC and two single layers (triangles up and triangles down).

Increased load and hydrogen utilization factor

As shown before, each layer of the developed hydrogen storage reactor was able to operate at steady state for an electric load of 160 W and 100 min. Furthermore, it has been shown that the design is scalable, thus the number of layers can be adapted to the actual load without affecting the reachable discharge state.

In this section, the effect of an increased load of the present setup has been studied in order to reveal the limits of the present design. Furthermore, the utilization factor of the stored hydrogen is discussed. Figure 6 shows the results for absorption and desorption of 2 layers with flow rates of 5.2 (RC), 10.5 (2*RC), 21 (4*RC), as well as 41.9 (8*RC) mgs^{-1}.

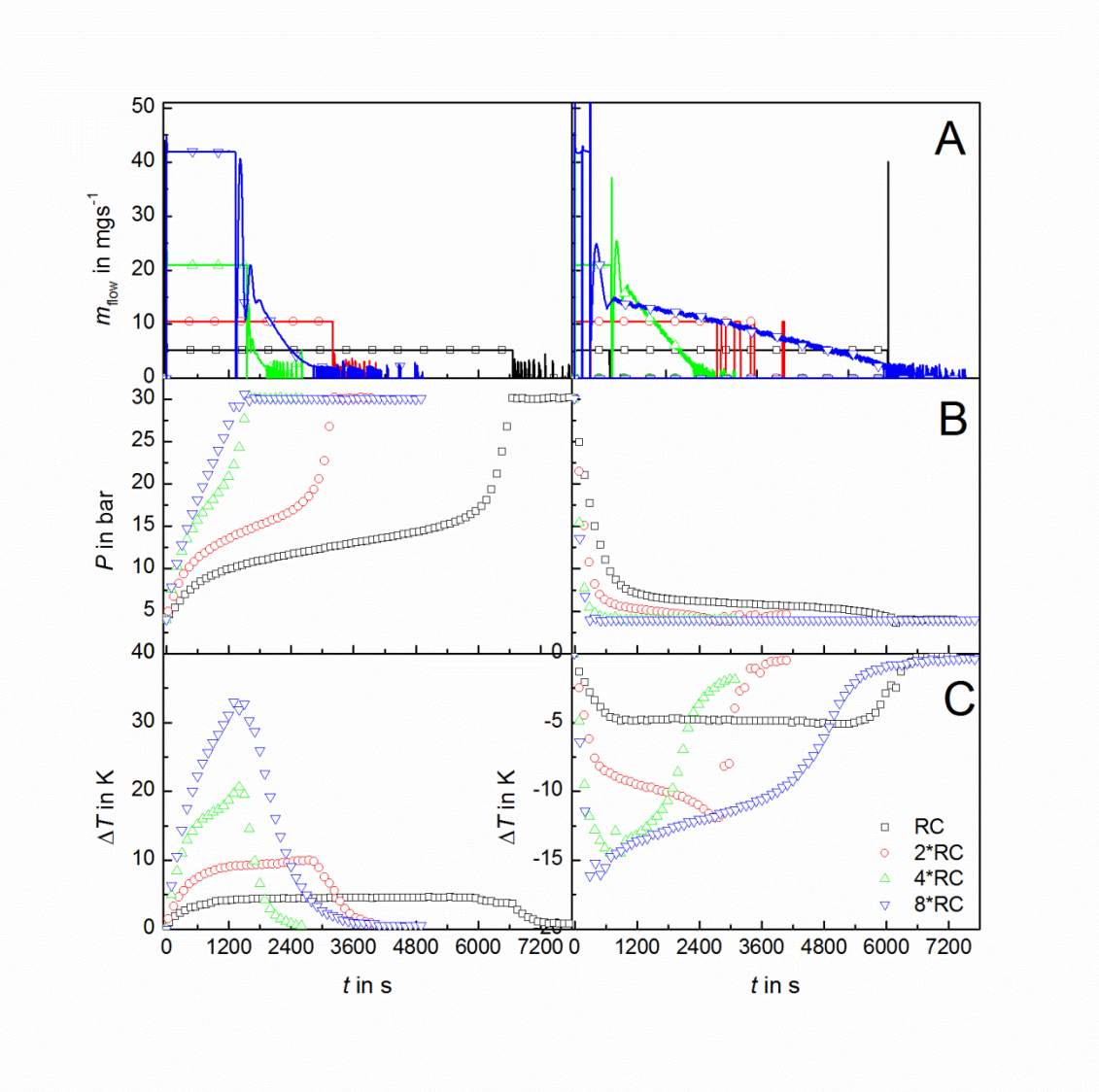

Figure 6: Mass flow rate (A), pressure (B) and temperature difference (C) versus time for absorption (left) and desorption (right) under RC, 2*RC, 4*RC, and 8*RC.

For absorption (left), the trends are as expected: The time interval with constant flow rates (A) scales almost linearly with the applied flow rate. Thus, for 2*RC 50 min, for 4* RC 25 min and for 8*RC about 13 min are reached. However, in order to reach the corresponding power loads for flow rates above 2*RC, the temperature in the reactor does not reach a steady state anymore, but it continuously increases – indicating that heat transport is limiting even at $\Delta T > 25$ K. Corresponding to the thermodynamics of the material, not only the temperatures inside of the material, but also the pressures increase and for the higher rates basically no plateau is appearing.

For the desorption process (right), even for loads with 2*RC it was not possible to deliver sufficient hydrogen at pressures above 4 bar. As it can be seen in Figure 6 (A, right), the time interval with a constant flow rate of hydrogen for 2*RC reaches less than the required 3000 s. This can be explained by the corresponding temperature and pressure plots. As the temperature decreases by more than

10 K (red circles), the equilibrium pressure decreases below the required 4 bar back pressure. For higher flow rates the behavior is even more pronounced.

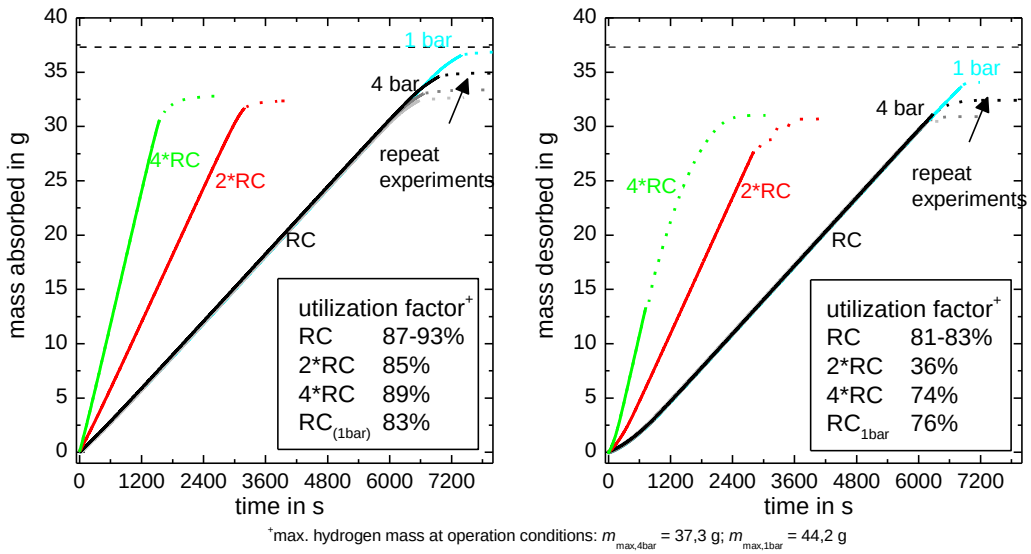

Figure 7: Mass absorbed (left) and mass desorbed (right) versus time for repeated experiments at RC (light grey, grey, black), 2*RC (red), 4*RC (green), and RC starting/ending at 1 bar instead of 4 bar (turquoise).

Next to the discussion of the experimental observations in Figure 6, Figure 7 shows the calculated hydrogen mass absorbed (left) or desorbed (right) during the same experiments. Using these data, it is possible to discuss the actual utilization factor of the stored hydrogen that has been reached at the different flow rates. As long as the mass flow rate is constant, the evolution of the hydrogen mass is represented with straight lines, and as soon as the mass flow rate decreases the evolution of the absorbed/desorbed mass is shown with dots. All values are already reduced by the amount of hydrogen stored in the void volume of 0.90×10^{-3} m^3 at the exact experimental conditions (on average this refers to about 2 g hydrogen).

For the experiment at RC, three repeated experiments are shown (light grey to black). All the corresponding graphs show exactly the same slope, and towards the end, for a higher cycling number a slightly higher mass of hydrogen can be absorbed. This indicates that the capacity is still slightly increasing with the cycles. In the last experiment at RC (black), a final value of 34.6 g absorbed hydrogen is reached at constant flow rate. This value refers to a very good utilization factor of 93 %, when at the experimental conditions starting from 4 bar and reaching 30 bar at 25 °C a maximum hydrogen mass of 37.3 g (1.31 wt.%, grey dashed line) is calculated. In case the experiment at RC conditions is extended starting from a pressure of 1 bar instead of 4 bar (turquoise), the absorption time is extended by 8.8% reaching a final mass of 36.6 g of hydrogen. However, under these conditions a storage capacity of 1.55 wt% resulting in 44.2 g would theoretically be feasible leading to a utilization factor of 83%. As discussed before, for the experiments with 2*RC and 4*RC, the

absorption time at constant flow rate decreases - as expected - to times of almost ½ and ¼. Therefore, it is clear that also the utilization factor for 4*RC is only reduced to 82% in comparison to 93% for RC.

For desorption, it could be observed that all final values are approx. 2 g lower than for desorption. The reason for this behavior is in the experimental setup, where in the first seconds starting at high pressure the mass flow meter is not able to measure the correct values. Therefore, the trends are still obvious, but for the utilization factor lower values are calculated. In the repeated experiments (grey to black) the same effects as for absorption can be observed: during cycling the amount of hydrogen increases and for the extension to 1 bar more hydrogen is released (turquoise). In case of an increasing flow rate of 2*RC (red) and 4*RC (green), however, it is obvious that the utilization factor of the stored hydrogen at constant flow rate is significantly decreasing and for 2*RC and 4*RC values of 74%, and 36%, respectively, are calculated compared to 83% at RC.

The reason in the strong decline of the utilization factor for higher flow rates during desorption in contrast to absorption can be explained by Figure 2. As mentioned in the beginning, the temperature difference between the nominal operational temperature and the equilibrium temperature was 10 K for absorption and desorption. However, in this graph, the assumption for the nominal ambient temperature was between 15 °C and 40 °C. Since the experiments were performed with ambient air at an ambient temperature of around 20 °C, the absorption reaction was thermodynamically favored at the current experimental conditions.

At this point it can be summarized that the modular tank design with a simple thermal management is able to combine constant mass flow rates with a high hydrogen utilization factor – at RC. If the load is increased to higher values, the temperature and pressure profiles get highly dynamic and especially for desorption the load cannot be provided until the storage reactor is fully depleted. Thus, in case higher loads are required, a modular scale-up of the reaction is necessary, e.g. the number of layers should be increased. However, this will not only increase the possible hydrogen loads, but also the total amount of hydrogen stored. In case, the total amount of hydrogen should stay constant while the loads should be increased, it is obvious that a different design with thinner tube diameters is required in order to decrease the heat load per surface area.

Effect of electric fan

The last effect that has been studied is the impact of the fan on the performance of the reactor. As mentioned in the section on the system layout, the external heat transfer is more important for the reactor design with thicker tubes and MHC inside.

Figure 8 depicts the resulting temperature and pressure profiles for the reference absorption experiment with fan (black) and without fan (turquoise). The temperature clearly indicates that the heat transfer between air and the tube is significantly reduced when the fan is switched off, as the temperature continuously decreases to less than 10 °C. After around 2400 s the pressure in the tank reaches 4 bar (indicated by arrow) and the required mass flow of hydrogen cannot be provided. At this time clearly no steady state has been reached and only 10.2 g of hydrogen are desorbed. Concluding, it can be stated that the fans are strictly required to guarantee the desired performance. However, with their electric power consumption of about 1.7 W per layer this effort seems reasonable.

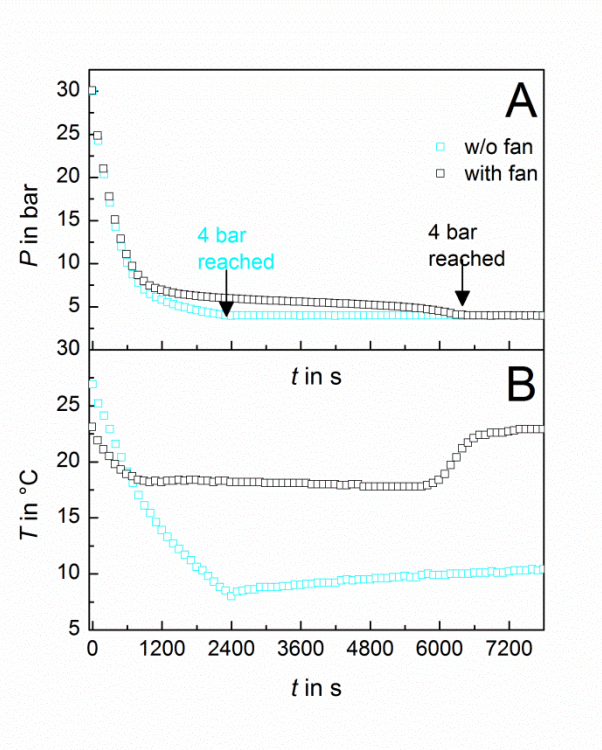

Figure 8: Pressure (A) and temperature difference (B) versus time for desorption experiment at RC with fan and without fan.

5 Conclusion

In the present publication a standardized metal hydride buffer hydrogen storage reactor is presented that focusses on two aspects for a simple system: selection of a storage material able to operate near ambient conditions and a simple heat transfer design using MHC as well as air as heat transfer fluid. The main objective was to investigate the operational characteristics of such a tank with regard to the utilization factor of the stored hydrogen for given charging and discharging rates.

The reactor consists of 4 identical layers that are designed to provide sufficient hydrogen for 100 min of fuel cell operation at 160 W_{el} using MHC at ambient temperatures between 10 °C and 40 °C. The

experimental results demonstrate that it is possible to operate this reactor at the load of this reference case at steady-state with a temperature difference between ambient and reaction of approximately 5 K. Furthermore, it has been shown that the modular system is scalable thus that single tube layers operate independently. The effect of an increased load on the present system for absorption and desorption is also presented using loads that are a factor of 2, 4 and 8 higher. It is shown that for absorption at RC a very high utilization factor of the stored hydrogen of 93 % can be achieved, that is only reduced to 89% when the flow rate is increased to 4*RC. For desorption at RC, a slightly lower utilization factor of 83 % is calculated due to the measuring setup and due to the operating conditions this value is even reduced to 36 % for 4*RC. Finally, the experimental results reveal that electric fans are crucial for the overall performance as they significantly influence the heat transfer from the reactor tube to the air. With 30 kg the laboratory system is currently too heavy, however using improved assembly techniques it will be possible to reduce the weight by 50 %.

Summarizing, a solid-state hydrogen storage tank with simple design and little heat transfer effort was presented that is able to reach high utilization factors of around 90 %.

Acknowledgements

This work is financially supported by the German Federal Ministry of Education and Research (BMBF) within the project Highly Dynamic Hydride-Graphite Composites (HD-HGV) (grant number 03EK3020). The authors want to thank Maximilian Marschall and Philipp Golebniak for their contributions to reactor design and measurements of the tank.

References

[1] G. Saur, Wind-To-Hydrogen Project : Electrolyzer Capital Cost Study, NREL/TP-550-44103, 2008. doi:10.2172/944892.

[2] G. Friedlmeier, A. Manthey, M. Wanner, M. Groll, Cyclic stability of various application-relevant metal hydrides, J. Alloys Compd. 231 (1995) 880–887. doi:10.1016/0925-8388(95)01776-3.

[3] M. Wanner, G. Friedlmeier, G. Hoffmann, M. Groll, Thermodynamic and structural changes of various intermetallic compounds during extended cycling in closed systems, J. Alloys Compd. 253-254 (1997) 692–697. doi:10.1016/S0925-8388(96)03041-1.

[4] B. Sakintuna, F. Lamari-Darkrim, M. Hirscher, F. Lamaridarkrim, Metal hydride materials for

solid hydrogen storage: A review, Int. J. Hydrogen Energy. 32 (2007) 1121–1140. doi:10.1016/j.ijhydene.2006.11.022.

[5] B. Delhomme, A. Lanzini, G. a. Ortigoza-Villalba, S. Nachev, P. de Rango, M. Santarelli, P. Marty, P. Leone, Coupling and thermal integration of a solid oxide fuel cell with a magnesium hydride tank, Int. J. Hydrogen Energy. 38 (2013) 4740–4747. doi:10.1016/j.ijhydene.2013.01.140.

[6] P. Marty, P. de Rango, B. Delhomme, S. Garrier, Various tools for optimizing large scale magnesium hydride storage, J. Alloys Compd. 8388 (2013). doi:10.1016/j.jallcom.2013.02.169.

[7] M. Hagstrom, Metal hydride hydrogen storage for near-ambient temperature and atmospheric pressure applications, a PDSC study, Int. J. Hydrogen Energy. 20 (1995) 897–909. doi:10.1016/0360-3199(95)00025-9.

[8] M. V. Lototskyy, M.W. Davids, I. Tolj, Y. V. Klochko, B.S. Sekhar, S. Chidziva, F. Smith, D. Swanepoel, B.G. Pollet, Metal hydride systems for hydrogen storage and supply for stationary and automotive low temperature PEM fuel cell power modules, Int. J. Hydrogen Energy. (2015). doi:10.1016/j.ijhydene.2015.01.095.

[9] G. Capurso, B. Schiavo, J. Jepsen, G. Lozano, T. Klassen, M. Dornheim, Development of a modular room-temperature hydride storage system for vehicular applications, Appl. Phys. A. 236 (2016) 1–11. doi:10.1007/s00339-016-9771-x.

[10] C. Bossi, a. Del Corno, M. Scagliotti, C. Valli, Characterisation of a 3 kW PEFC power system coupled with a metal hydride H2 storage, J. Power Sources. 171 (2007) 122–129. doi:10.1016/j.jpowsour.2006.11.006.

[11] A. Nakano, H. Ito, T. Maeda, T. Munakata, T. Motyka, C. Corgnale, S. Greenway, J.M. Perez-Berrios, Study on a metal hydride tank to support energy storage for renewable energy, J. Alloys Compd. 580 (2013) S418–S422. doi:10.1016/j.jallcom.2013.03.152.

[12] Z. Liu, Y. Li, Q. Bu, C.J. Guzy, Q. Li, W. Chen, C. Wang, Novel fuel cell stack with coupled metal hydride containers, J. Power Sources. 328 (2016) 329–335. doi:10.1016/j.jpowsour.2016.07.096.

[13] T. Maeda, T. Fuura, I. Matsumoto, Y. Kawakami, M. Masuda, Cyclic stability test of AB2 type (Ti, Zr)(Ni, Mn, V, Fe)2.18 for stationary hydrogen storage in water contaminated hydrogen, J. Alloys Compd. 580 (2013) S255–S258. doi:10.1016/j.jallcom.2013.03.230.

[14] M. Dieterich, C. Pohlmann, I. Bürger, M. Linder, L. Röntzsch, Long-term cycle stability of metal hydride-graphite composites, Int. J. Hydrogen Energy. (2015).

doi:10.1016/j.ijhydene.2015.09.013.

[15] C. Pohlmann, L. Röntzsch, F. Heubner, T. Weißgärber, B. Kieback, Solid-state hydrogen storage in Hydralloy–graphite composites, J. Power Sources. 231 (2013) 97–105. doi:10.1016/j.jpowsour.2012.12.044.

[16] M. Ron, The normalized pressure dependence method for the evaluation of kinetic rates of metal hydride formation/decomposition, J. Alloys Compd. 283 (1999) 178–191. doi:10.1016/S0925-8388(98)00859-7.

[17] K. Herbrig, L. Röntzsch, C. Pohlmann, T. Weißgärber, B. Kieback, Hydrogen storage systems based on hydride–graphite composites: computer simulation and experimental validation, Int. J. Hydrogen Energy. (2013) 1–11. doi:10.1016/j.ijhydene.2013.03.104.

[18] J. Mitzel, E. Gülzow, A. Kabza, J. Hunger, S.S. Araya, P. Piela, I. Alecha, G. Tsotridis, Identification of critical parameters for PEMFC stack performance characterization and control strategies for reliable and comparable stack benchmarking, Int. J. Hydrogen Energy. 41 (2016) 21415–21426. doi:10.1016/j.ijhydene.2016.08.065.

[19] M. V. Lototskyy, I. Tolj, A. Parsons, F. Smith, C. Sita, V. Linkov, Performance of electric forklift with low-temperature polymer exchange membrane fuel cell power module and metal hydride hydrogen storage extension tank, J. Power Sources. 316 (2016) 239–250. doi:10.1016/j.jpowsour.2016.03.058.

[20] S. Suda, Y. Komazaki, N. Kobayashi, Effective thermal conductivity of metal hydride beds, J. Less Common Met. 89 (1983) 317–324. doi:10.1016/0022-5088(83)90340-5.

[21] F.S. Yang, G.X. Wang, Z.X. Zhang, X.Y. Meng, V. Rudolph, Design of the metal hydride reactors - A review on the key technical issues, Int. J. Hydrogen Energy. 35 (2010) 3832–3840. doi:10.1016/j.ijhydene.2010.01.053.

[22] P. Muthukumar, M. Groll, Metal hydride based heating and cooling systems: A review, Int. J. Hydrogen Energy. 35 (2010) 3817–3831. doi:10.1016/j.ijhydene.2010.01.115.

[23] M. Linder, R. Mertz, E. Laurien, Experimental results of a compact thermally driven cooling system based on metal hydrides, Int. J. Hydrogen Energy. 35 (2010) 7623–7632. doi:10.1016/j.ijhydene.2010.04.184.

[24] C. Pohlmann, L. Röntzsch, T. Weißgärber, B. Kieback, Heat and gas transport properties in pelletized hydride–graphite-composites for hydrogen storage applications, Int. J. Hydrogen Energy. 38 (2012) 1685–1691. doi:10.1016/j.ijhydene.2012.09.159.

[25] I. Bürger, M. Bhouri, M. Linder, Considerations on the H2 desorption process for a

combination reactor based on metal and complex hydrides, Int. J. Hydrogen Energy. 40 (2015) 7072–7082. doi:10.1016/j.ijhydene.2015.03.136.

[26] K. Herbrig, C. Pohlmann, Ł. Gondek, H. Figiel, N. Kardjilov, A. Hilger, I. Manke, J. Banhart, B. Kieback, L. Röntzsch, Investigations of the structural stability of metal hydride composites by in-situ neutron imaging, J. Power Sources. 293 (2015) 109–118. doi:10.1016/j.jpowsour.2015.05.039.

Table1

Table 1: Summary of properties for powder or MHC material as well as calculated design parameters (materials properties taken from [17]).

	Hydralloy® powder	Hydralloy®-based MHC
	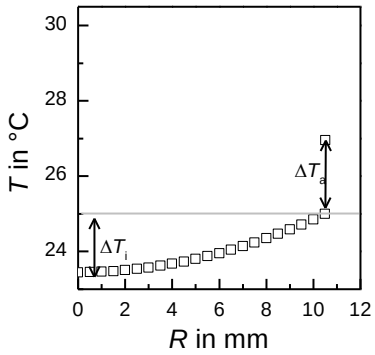	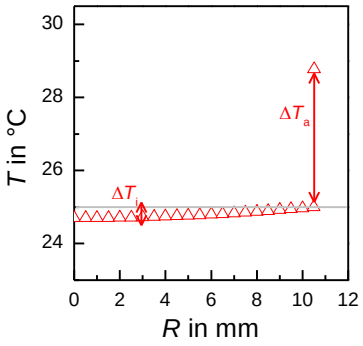
Req. power in W_{el} per layer	160	160
ρ in kgm^{-3}	2000	4040
λ in $Wm^{-1}K^{-1}$	1	9.9
***m* in kg**	1.35	1.42
***L* in m**	1.95	1.01
***Q/A* in Wm^{-2}**	295	567
***Q/V* in kWm^{-3}**	56.3	108.3
ΔT_i in K	1.55	0.30
ΔT_a in K	1.96	3.78

Table2

Table 1: Photograph of storage tank demonstrator and its main features.

Mass MHC in kg	6
Total mass in kg	30
Stored volume of H_2 in m^3	1
Designed load in W_{el} per layer	160 for 100 min, @ 4 bar back pressure
Dimensions in mm	261 × 444 × 458

Figure1

Click here to download high resolution image

Figure2

Click here to download high resolution image

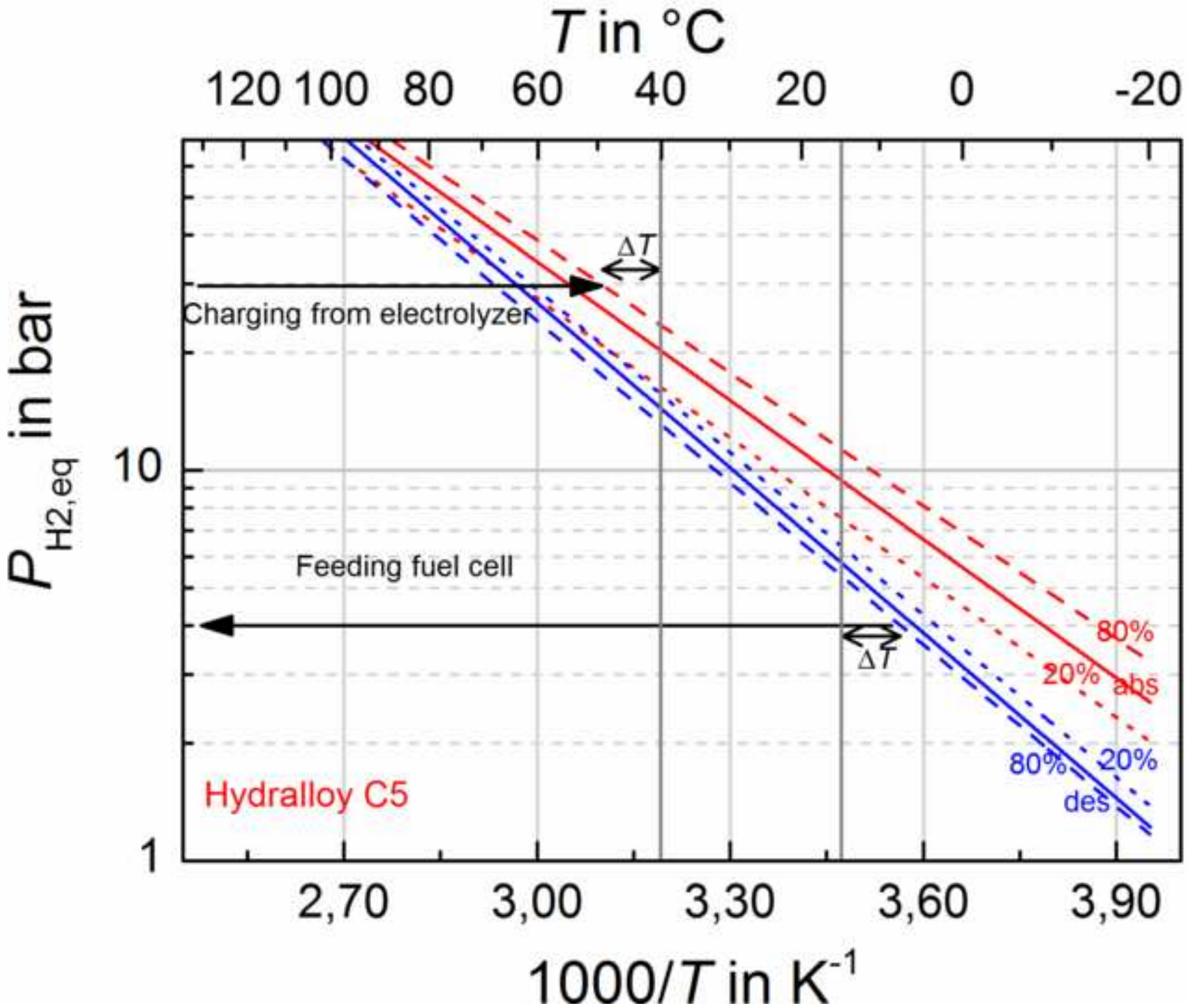

Figure3

Click here to download high resolution image

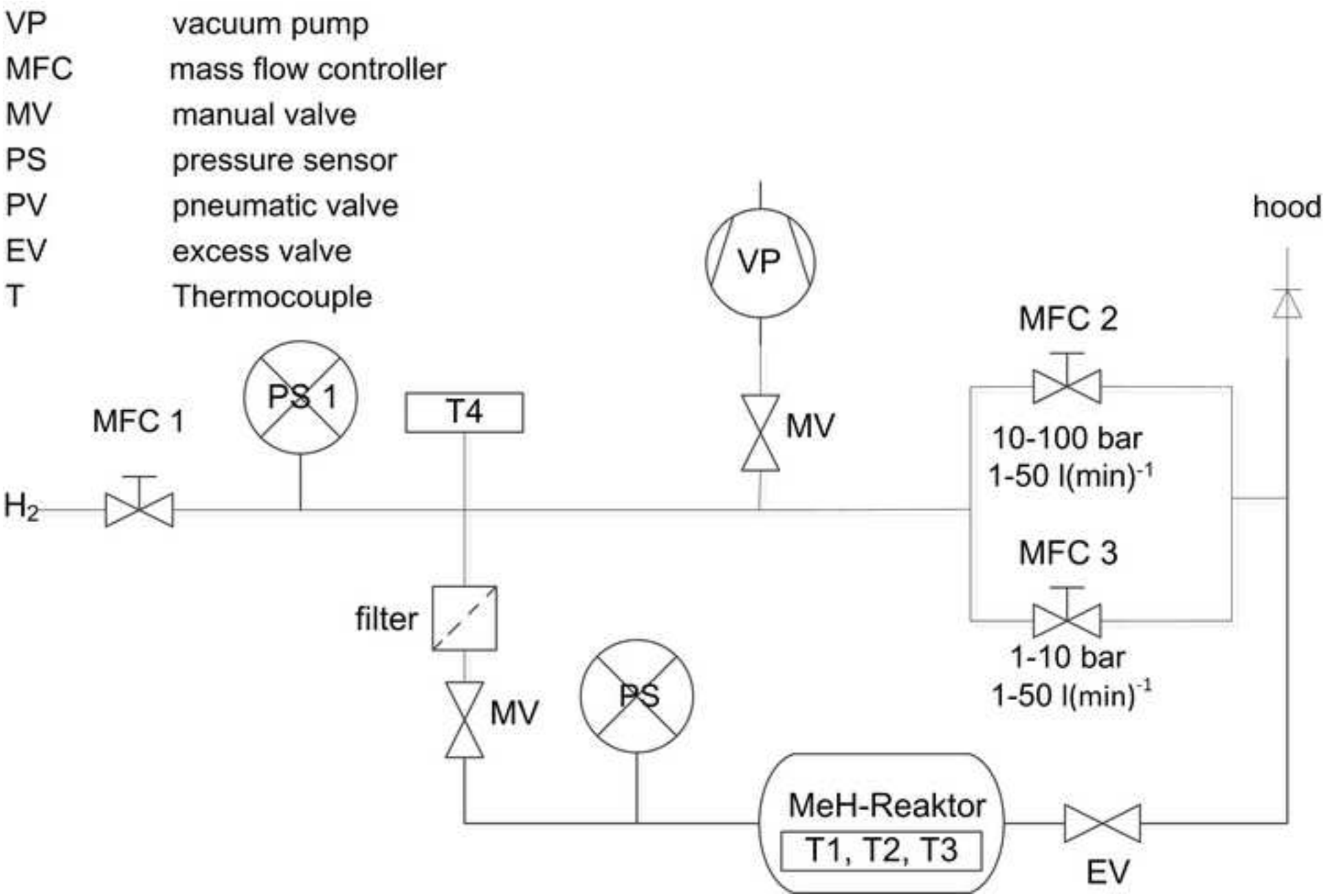

Figure4

Click here to download high resolution image

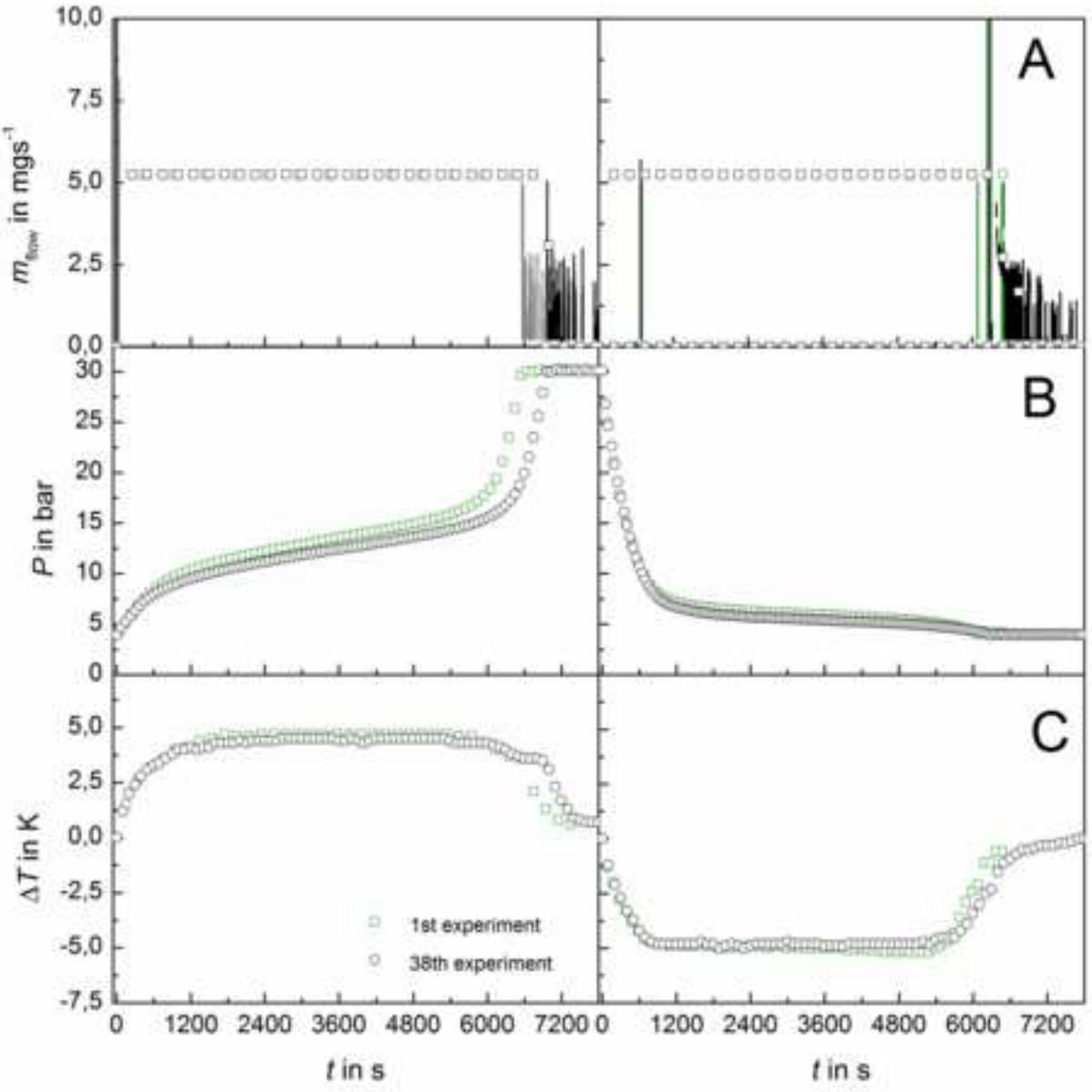

Figure5

Click here to download high resolution image

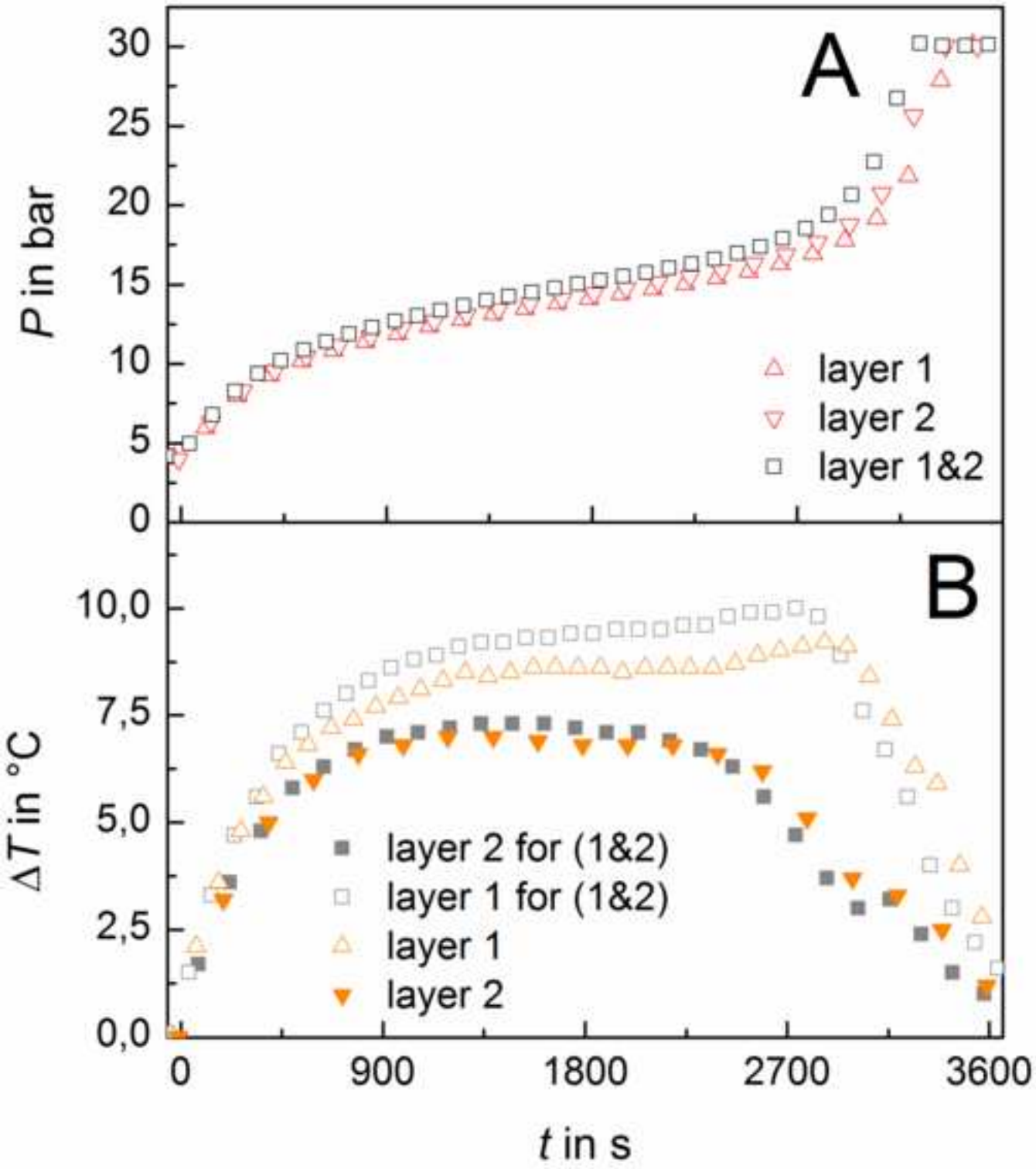

Figure6

Click here to download high resolution image

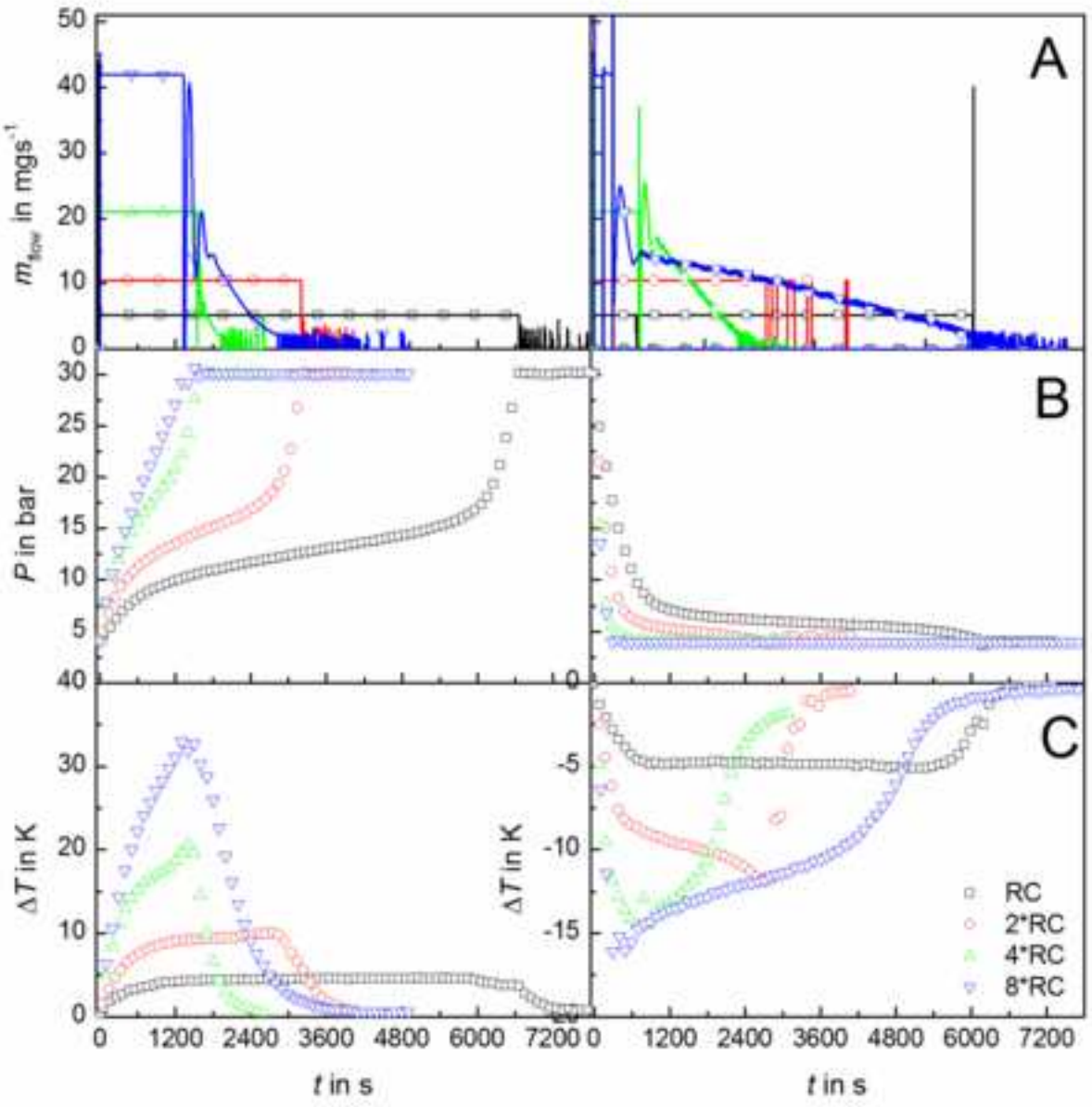

Figure7

Click here to download high resolution image

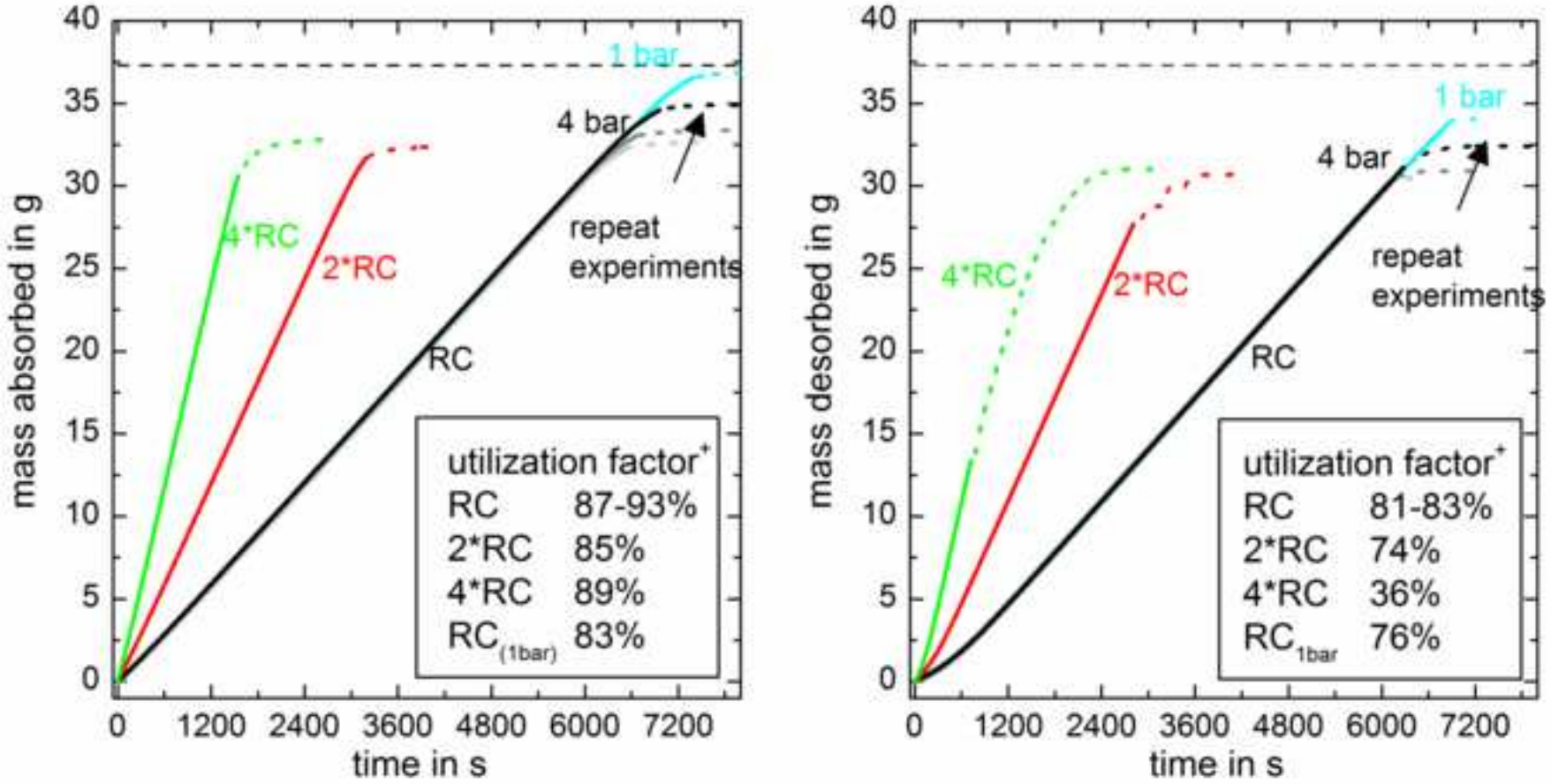

*max. hydrogen mass at operation conditions: $m_{max,4bar}$ = 37,3 g; $m_{max,1bar}$ = 44,2 g

Figure8
Click here to download high resolution image

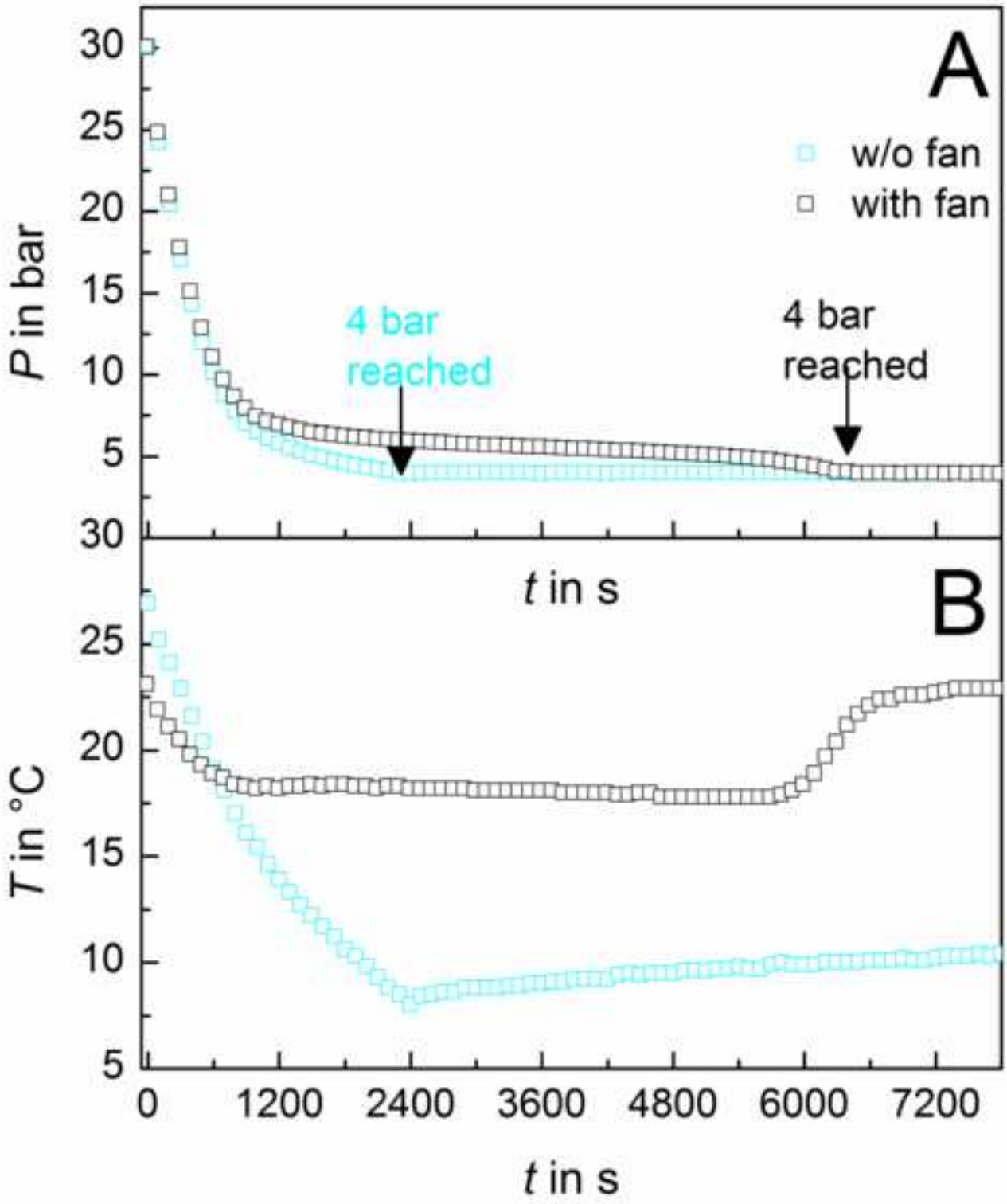

Figure 1: Scheme of a hydrogen-based power2gas system to store surplus electrical power.

Figure 2: Van´t hoff plot of Hydralloy C5 [16]**, and operation conditions for the present reactor design.**

Figure 3: Test rig layout.

Figure 4: Mass flow rate (A), pressure (B) and temperature difference (C) versus time for absorption (left) and desorption (right) under RC.

Figure 5: Pressure (A) and temperature difference (T1: full and T2: open symbols, B) versus experimental time with 2*RC and 2 layers (squares) as well as with 2*RC and two single layers (triangles up and triangles down).

Figure 6: Mass flow rate (A), pressure (B) and temperature difference (C) versus time for absorption (left) and desorption (right) under RC, 2*RC, 4*RC, and 8*RC.

Figure 7: Mass absorbed (left) and mass desorbed (right) versus time for repeated experiments at RC (light grey, grey, black), 2*RC (red), 4*RC (green), and RC starting/ending at 1 bar instead of 4 bar (turquoise).

Figure 8: Pressure (A) and temperature difference (B) versus time for desorption experiment at RC with fan and without fan.

Table 1: Summary of properties for powder or MHC material as well as calculated design parameters (materials properties taken from [17]).

Table 2: Photograph of storage tank demonstrator and its main features.